

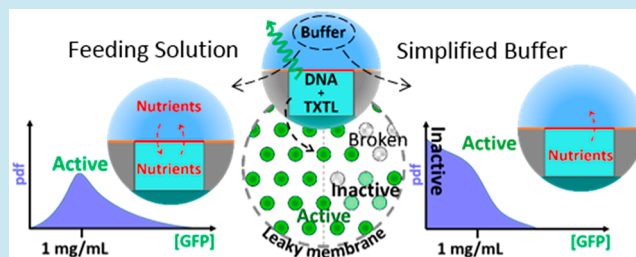
## Gene Expression in on-Chip Membrane-Bound Artificial Cells

Ziane Izri,<sup>\*,†</sup> David Garenne,<sup>‡</sup> Vincent Noireaux,<sup>‡,ⓑ</sup> and Yusuke T. Maeda<sup>†</sup><sup>†</sup>Department of Physics, Kyushu University, Fukuoka, 819-0395, Japan<sup>‡</sup>School of Physics and Astronomy, University of Minnesota, Minneapolis, Minnesota 55455 United States

## Supporting Information

**ABSTRACT:** Artificial cells made of molecular components and lipid membrane are emerging platforms to characterize living systems properties. Cell-free transcription–translation (TXTL) offers advantages for the bottom-up synthesis of cellular reactors. Yet, scaling up their design within well-defined geometries remains challenging. We present a microfluidic device hosting TXTL reactions of a reporter gene in thousands of microwells separated from an external buffer by a phospholipid membrane. In the presence of nutrients in the buffer, microreactors are stable beyond 24 h and yield a few mg/mL of proteins. Nutrients in the external solution feed the TXTL reaction at the picoliter scale via passive transport across the phospholipid membrane of each microfluidic well, despite the absence of pores. Replacing nutrients with an inert polymer and fatty acids at an isotonic concentration reduces microreactors efficiency, and a significant fraction yields no protein. This emphasizes the crucial role of the membrane for designing cell-free TXTL microreactors as efficient artificial cells.

**KEYWORDS:** cell-free transcription–translation, microfluidics, passive trans-membrane transport



Constructing biochemical systems *in vitro* using molecular components is a powerful approach to understand living systems. This requires a tunable experimental platform that reproduces the key features of the living systems. One of the most essential sets of biochemical reactions in living organisms is the synthesis of proteins achieved through gene expression.<sup>1</sup> It can now be efficiently performed *in vitro* in cell-free transcription–translation (TXTL) systems.<sup>2,3</sup> A cytoplasmic extract provides the molecular machinery necessary to recapitulate transcription and translation,<sup>4–6</sup> to which engineered linear or circular DNAs are added to execute gene circuits. This method, highly versatile compared to *in vivo* approaches, enables rapid prototyping of regulatory parts and elementary gene circuits, and has become a common procedure to study biological systems *in vitro*, from gene expression<sup>7–9</sup> to self-organization<sup>10,11</sup> and metabolism.<sup>12</sup>

Compartmentalization is an essential feature of living cells. It allows separating the intracellular medium from its environment as well as developing the functions that enable interactions with that environment. Liposomes are typically used to make TXTL-based artificial reactors because they resemble living cells albeit with much less integrated molecular functions.<sup>3,7,8,10,11</sup> Although durable cell-free gene expression has been achieved in liposomes, it is still not easy to accurately control their size distribution and further examine how the lipid interface affects internal TXTL reactions.

Microfluidic microreactors are highly suitable and convenient to host TXTL reactions because they can be easily made into a wide array of materials, with various sizes and shapes. Several systems have been developed to achieve robust gene expression in water-in-oil droplets,<sup>9</sup> circular microwells,<sup>13,14</sup>

and glass-etched microchannels.<sup>15,16</sup> Small chambers interconnected by narrow microchannels showed rich dynamical behaviors such as front wave propagation.<sup>17</sup> In spite of sophisticated advances in incorporating TXTL to microfluidic chips,<sup>18</sup> the lack of natural membrane boundary to properly mimic living systems is a limitation. It is still challenging to integrate a biological membrane within microfluidic reactors encapsulating TXTL system.

In this letter, we present a novel microfluidic system that allows efficient cell-free gene expression in picoliter-sized microwells carved into a substrate sealed on one side by a phospholipid membrane.<sup>19–21</sup> A reporter gene (deGFP) is expressed during more than 24 h in thousands of isolated microwells containing a TXTL reaction mix with an external solution containing the necessary resources (ribonucleosides, amino acids). The protein synthesis is on the order of 1.0 mg/mL of protein (39  $\mu$ M deGFP). The statistical analysis of protein synthesis over a large population reveals that the TXTL reaction confined in cell-sized microreactors sealed by a phospholipid membrane is sensitive to the composition of the outer medium. In particular, the absence of nutrients in the outer medium reduces the yield of the TXTL reaction and causes a significant fraction of the microreactors to be repressed. Sensitivity to the composition of an external buffer demonstrates the importance of passive transport across the phospholipid membrane of material necessary to the TXTL reaction.

Received: February 25, 2019

Published: July 3, 2019

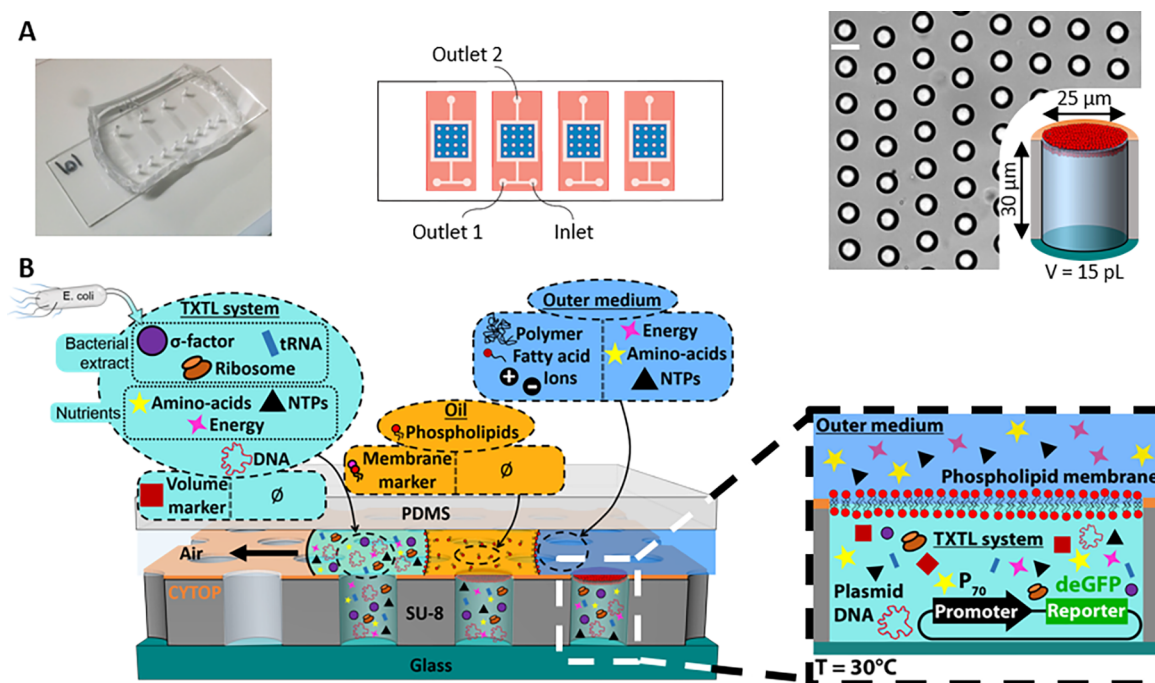


**Figure 1.** Microfluidic setup and cell-free TXTL reactions in microwells sealed with membrane. (A, left) Microfluidic chip used in this study. (A, middle) Four separate units made of SU-8 (blue) are microfabricated on top of a slide glass and closed by a PDMS cover (pink). (A, right) Bright field image of microwells and characteristic dimensions. Scale bar is  $25\ \mu\text{m}$ . (B) Preparation and molecular content of the microreactors. (B, left) The chamber is sequentially flushed with the TXTL reaction mix, the oil phase, and the buffer. After these three flushes, microreactors are sealed with a phospholipid membrane. (B, right) Individual microreactors typically contain TXTL reaction with plasmid DNA encoding  $P_{70a}$ -deGFP circuit as well as a volume marker (red fluorescent dye).

The chip we designed is made of two parts: a cover slide that hosts microwells carved into a  $30\ \mu\text{m}$  SU-8 layer spread on a glass cover slide, and a PDMS cover that closes the chip  $20\ \mu\text{m}$  above (Figure 1A left and middle). To ensure the stability of the membrane sealing, SU-8 is coated with CYTOP, a fluorinated coating agent.<sup>20,21</sup> The array of microwells contains about 5000 circular microwells with a radius of  $25\ \mu\text{m}$  and a typical volume of  $15\ \text{pL}$  (Figure 1A, right). Each microwell is a biochemical reactor that stands for a single artificial cell isolated from its environment. Although only  $\approx 60$  microwells can be continuously observed at once, the large number of microwells present in the array offers the possibility to explore a large statistics of end points.

Microwells are filled sequentially (Figure 1B left):<sup>20,21</sup> first, the TXTL reaction mix, containing crude *E. coli* extract and nutrients, supplemented with the plasmid  $P_{70a}$ -deGFP, and, when needed, the red fluorescent volume marker Rhodamine-BSA (molecular weight  $\approx 66\ \text{kDa}$ ), completely fills the chamber. Then, the oil phase that contains the mixture of phospholipids (DOPE and DOPG), and when needed, the red fluorescent membrane marker DOPE-ATTO-594 (labeled DOPE), is flushed through the chamber to remove the aqueous solution above the microwells and cover the microwells with a phospholipid monolayer. Finally, the external buffer, a feeding solution that has the same composition as the TXTL reaction mix, minus the crude *E. coli* extract and the plasmid DNA respectively replaced with S30B buffer and water,<sup>22</sup> flushes out the oil phase. As it moves across the chamber, the interface assembles both phospholipid monolayers into a membrane that seals the microwells.

To make sure that the microreactors are isolated from one another, we separately tested the diffusive recovery of

fluorescence after photobleaching (FRAP) of the volume (Figure 2A–C) and membrane (Figure 2D–F) markers. We found that the recovery of fluorescence in the microwells was negligible while the fluorescence in bulk recovered within few minutes (Figure 2B,E). Such absence of recovery shows, on the one hand, that the content of the microwells is properly sealed, because molecular diffusion from neighboring microwells and the leakage of large molecules into the buffer are negligible (Figure 2A–C). On the other hand, it shows that groups of microwells are not covered by large oil patches, but individually by single phospholipid membranes (Figure 2D–F).

To illustrate the working principle of the *on-chip* artificial cells, we performed constitutive expression of the gene coding for green fluorescent protein deGFP (molecular weight  $\approx 27\ \text{kDa}$ ), cloned under the  $P_{70a}$  promoter, at  $30\ ^\circ\text{C}$  (Figure 1B, right). Each microreactor contains about  $n \approx 4 \times 10^3$  plasmid DNA copies, with a relative variability of the order of  $1/\sqrt{n} \approx 2\%$ . Microreactors showed an increase of green fluorescence while the fluorescence of both volume marker (Figure 3A) and membrane marker (Figure 3B) remained constant. The profiles of the membrane thickness (Figure 3C), the height of reaction mix (Figure 3D), and the distribution of GFP produced in each microreactor (Figure 3C,D) all show a flat part at the center of the microwell, indicating the presence of a flat membrane. After 8 h, most of the microreactors are intact. We successfully observed cell-free gene expression inside microreactors with membrane sealing.

Although FRAP experiments showed that large molecules cannot cross the membrane, passive transport of smaller molecules, such as hydrophobic amino-acids, can occur across the phospholipid membrane.<sup>23</sup> To put into light the role of

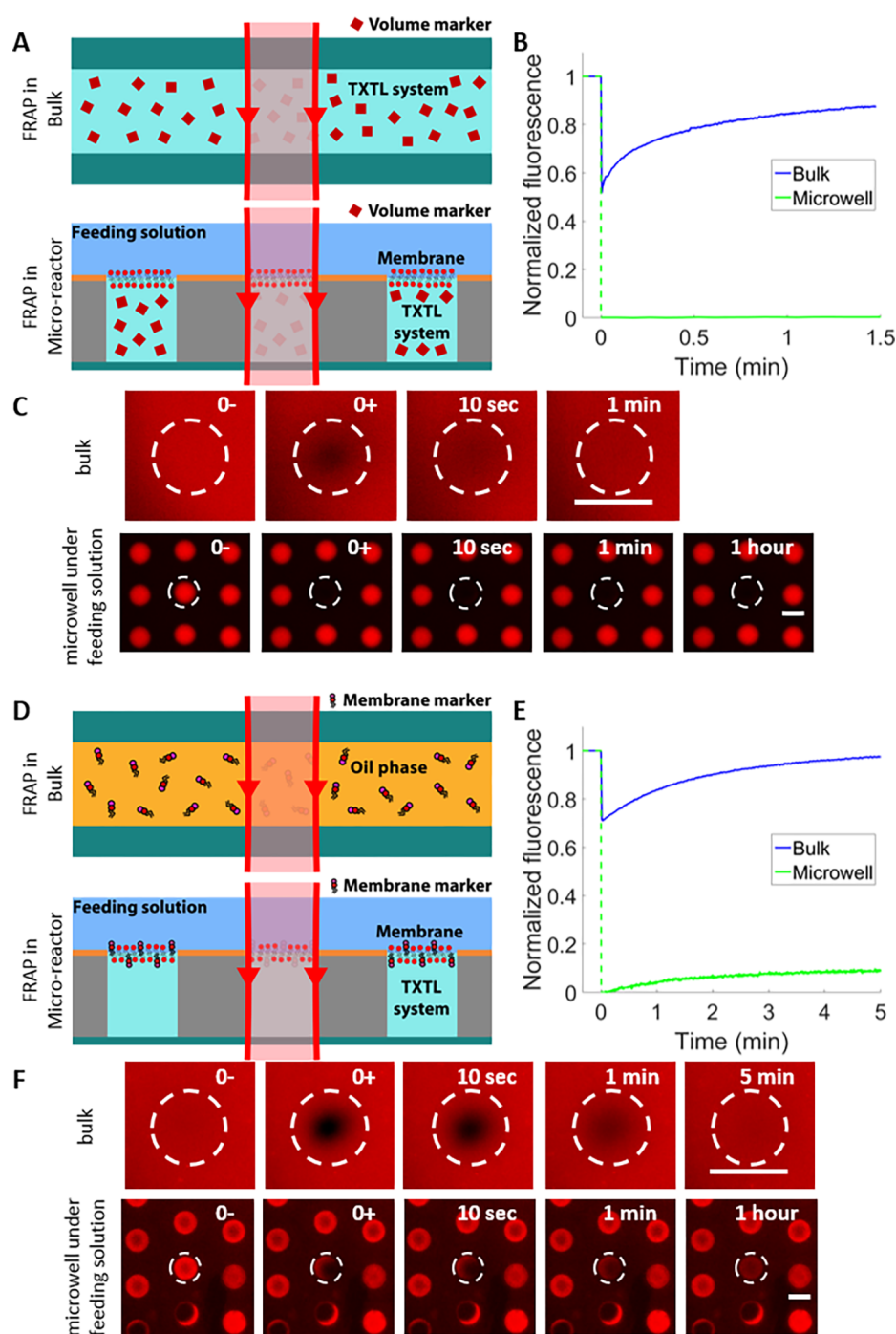


**Figure 2.** FRAP analysis to visualize insulation of microwells under feeding solution. (A) Leakage of the TXTL system from inside the microwells was tested with the FRAP analysis of the volume marker (Rhodamine-BSA) in the microwells (bottom). In the bulk FRAP experiment, the same thickness of TXTL system is achieved with a 30 μm spacer between two glass slides (top). (B) In the microwells (green solid line) it is less than a percent within 1.5 min while photobleached fluorescence recovers its initial intensity within a minute in the bulk solution (blue solid line). (C) Snapshots of FRAP of volume marker. In the top panel, the white dashed circle encloses the photobleached area in bulk conditions, while in the bottom panel, it encloses the only photobleached microwell in the array of microwells. (D) Insulation of the microwell membrane was tested with the FRAP analysis of the membrane marker (labeled phospholipid DOPE-ATTO-594) in the microwells (bottom). In the bulk FRAP experiment, the oil phase with membrane marker is enclosed between two glass slides separated by a 30 μm spacer (top). (E) In the microwells (green solid line), fluorescence recovery was less than a few percent within 5 min while it took about 5 min for it to recover its initial fluorescence intensity in the bulk solution (blue solid line). (F) Snapshots of FRAP of the membrane marker. Scale bars are 25 μm.

nutrients in the external buffer, two compositions were tested: the feeding solution and a simplified buffer with polymer<sup>24</sup> and fatty acid,<sup>25,26</sup> as well as ions. Osmotic flow across the membrane interface was balanced by adjusting the concentration of polymer to isotonic conditions. The concentration of

fatty acid was kept low enough to allow stable membrane growth under slight osmotic misbalance<sup>25,26</sup> (Supporting Information, Figure S1). Microreactors under simplified buffer show the same insulation properties as under feeding solution (Figure S2), and present qualitatively the same gene expression

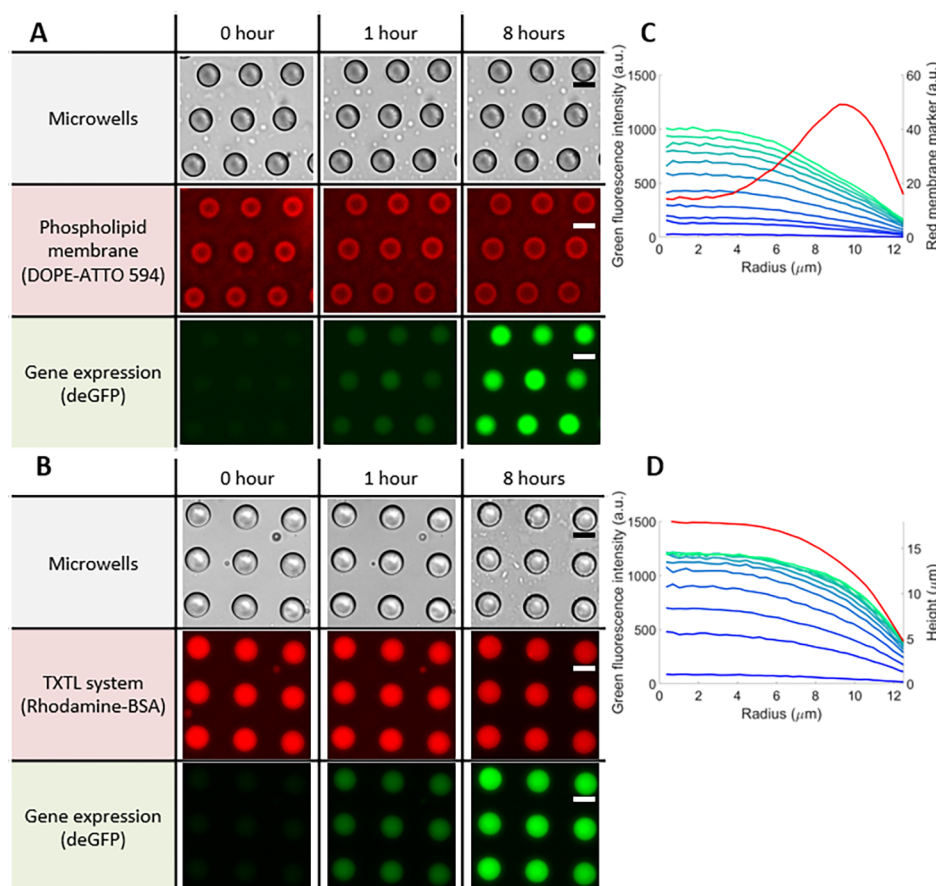


**Figure 3.** Typical observations of microreactors. (A and B) Snapshots over 8 h of TXTL reactions of deGFP synthesis under feeding solution. Phospholipid membrane is visible in bright field (A and B, top). Red fluorescence of microwells remains constant (A and B, middle). As cell-free gene expression proceeds, deGFP is synthesized and green fluorescence intensities in microreactors increases (A and B, bottom). (C and D) Radial distributions of green fluorescence intensity over 8 h of gene expression (from blue to green) as well as red fluorescence intensity (red), for membrane marker (C) and volume marker (D). Scale bars are 25  $\mu\text{m}$ .

kinetics trend as well as the same interface structure (Figure S3).

We then compared the kinetics of protein synthesis in microreactors kept under continuous observation for 24 h under feeding solution (Figure 4A) and simplified buffer (Figure 4B). Assuming that the rate of protein production is proportional to the concentration of remaining substrate (e.g., amino-acids), and that the deGFP degradation in the TXTL system is negligible,<sup>6</sup> one obtains the following kinetics law (see Supporting Information):

$$c(t) = c_{\infty} \left[ 1 - \exp\left(-\frac{t + t_0}{T}\right) \right] \quad (1)$$

where  $c(t)$  is the concentration of synthesized deGFP at time  $t$ ,  $T$  is the reaction time constant of the TXTL reaction, and  $t_0$  is the lag-time. Under both external buffers, the normalized kinetics of deGFP synthesis of all the microwells observed falls into the same master curve that agrees well with eq 1 (Figure 4C,D). Parameters extracted from curve fitting show that the yield of protein synthesis is independent of the reaction time  $T$  under feeding solution (Figure S5A), while it increases with  $T$  under simplified buffer (Figure S5B). Protein synthesis is also twice shorter under simplified buffer than under feeding solution. This can be explained by the gene expression in the cell-free extract with leaky membrane. Abundant chemical species in the feeding solution nullify the leak of permeating

species from the cell-free extract so that only the depletion of nonpermeating species as a result of gene expression is observed. In contrast, membrane sealing with a leak affects gene expression under simplified buffer by shortening its reaction time and lowering its yield.

During the same observation time, under simplified buffer, the number of microreactor membranes that break is significantly larger than that under feeding solution (Figure 4E,F). Although their volume has a low variability over the continuously observed sample of microreactors under simplified buffer, and remains constant, their lifetime presents a large variability (Figure 4G). This suggests that the initial volume of the reactor has no influence on the behavior of the membrane. In contrast, the yield of synthesized protein slightly increases with the lifetime of the membrane (Figure 4H), which suggests that more stable membranes are also less permeable to nutrients and thus thicker.

The presented device takes statistics over a large number of identical reaction mixes sealed by a membrane, as a clonal population of artificial cells. This allowed us to analyze the distribution of the yield of deGFP synthesis over all the microwells inside a chip still sealed after 24 h of gene expression. Figure 5 panels A and B show a clear difference between distributions of protein synthesis under feeding solution and under simplified buffer. Under feeding solution, it presents a typical yield of 1.0 mg/mL, consistent with

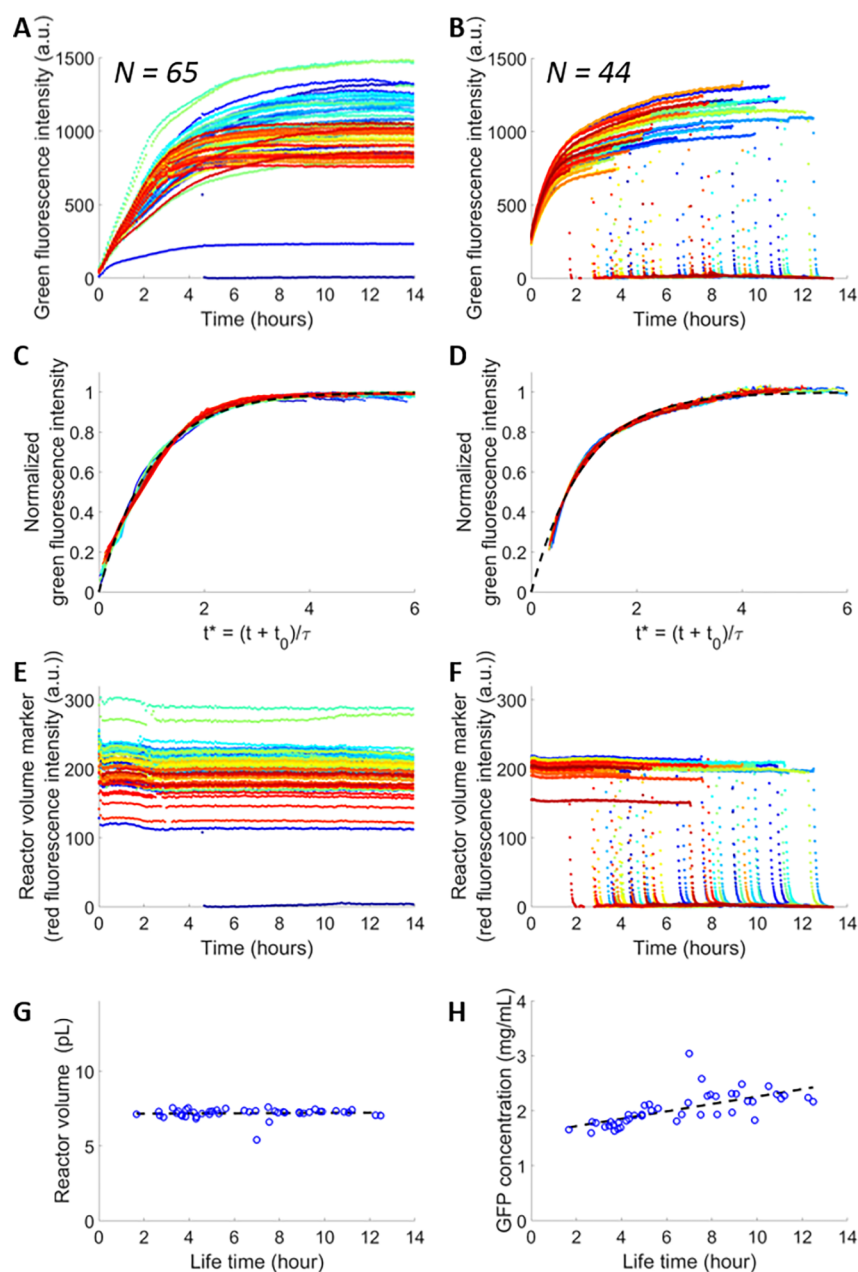


**Figure 4.** Quantitative analysis of cell-free TXTL reactions in active microreactors kept under continuous observation. (A,B) Traces of synthesized deGFP fluorescence intensity, displayed on natural axes, under feeding solution (A) and simplified buffer (B). Each color stands for a single microreactor.  $N$  counts the number of microreactors present. (C,D) Once rescaled by parameters  $c_{\infty}$ ,  $t_0$ , and  $T$  extracted from exponential fit, all the kinetics fall on the same master curve (black dashed line). (E,F) Traces of red fluorescence intensity of volume marker remain constant until membrane breaks. (E, feeding solution) Only one membrane rupture was observed during the continuous acquisition under feeding solution. (F, simplified buffer) However, membranes are less stable under simplified buffer. (G) Under simplified buffer, the initial volume of the microreactor has no effect on the stability of the membrane. (H) Although small, there is a positive correlation between the final GFP concentration and the lifetime of the membrane, which indicates that more durable membranes go with more efficient protein synthesis. Affine fit is represented in black dashed line.

previous work done in TXTL systems.<sup>4,5,22</sup> A broad tail stretches to the right (Figure 5A). However, that tail is absent under simplified buffer (Figure 5B). A significant proportion of intact microreactors under simplified buffer presents very low protein synthesis, whereas all the microreactors under feeding solution are active. As proteins are made of the assembly of nutrients, their abundance directly affects the yield of protein synthesis. In the absence of nutrients in the buffer, leakage prevents protein synthesis from reaching higher yields (Figure 5C).

Membranes obtained under simplified buffer are thinner than those obtained under feeding solution (Figure S5), which causes their increased permeability and their sensitivity to osmotic misbalance, resulting in a lower stability. Membrane thickness is not uniform among microreactors as its distribution presents a large standard deviation (Figure S5). This is expected to affect gene expression yield under simplified buffer, as membrane permeability is lower for thicker membranes.<sup>23</sup> The gene expression under feeding solution should however be unaffected by membrane thickness,

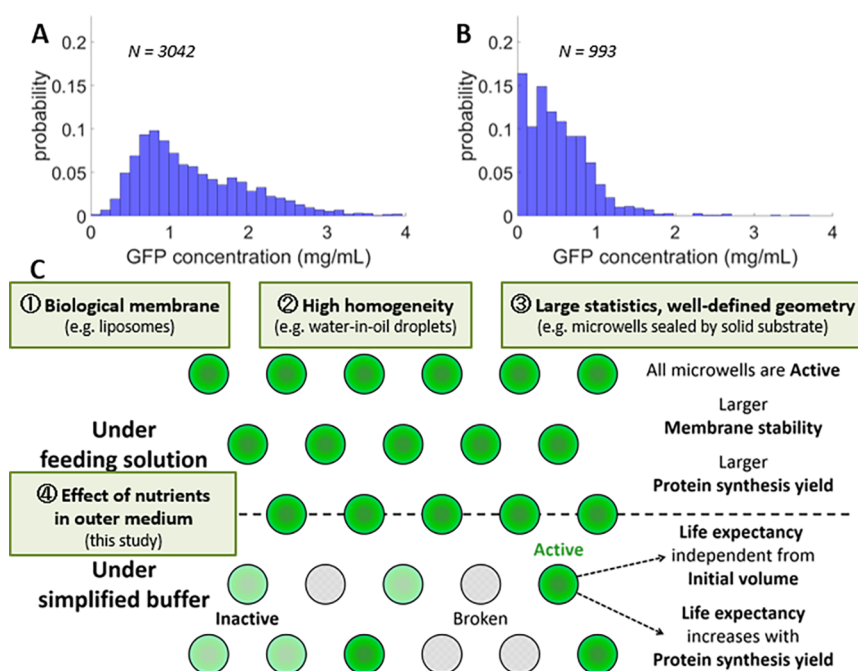


**Figure 5.** (A and B) Statistics of protein synthesis yield confined in microwells sealed by intact membrane after 24 h of gene expression under feeding solution (A) and under simplified buffer (B).  $N$  represents the total number of surviving microreactors after 24 h. (A) Under feeding solution, typical yield is 1.0 mg/mL of deGFP and can reach as high as 4.0 mg/mL. All microreactors are active. (B) On the contrary, under simplified buffer, yield is limited to 1.0 mg/mL and a significant fraction of microreactors have a yield close to 0 mg/mL. (C) Schematic illustration of the properties and advantages of the designed chip. Gene expression in on-chip membrane-bound microwells occurs (1) with a biological membrane similar to liposomes, (2) with highly homogeneous compartments as emulsions, and (3) in large statistics with well-defined geometry as solid microwells. By combining all of these technical advantages, this powerful microreactor was realized thanks to quantitative analysis of (4) the effect of the presence of nutrients in the outer medium on gene expression. In particular, under feeding solution, membranes are more stable, and microreactors are always active and reach a higher protein synthesis yield than under simplified buffer. The rich chemical energy of the feeding solution suppresses the leak of small hydrophobic chemicals occurring during protein synthesis.

as it is the nonpermeating species inside the microreactors that limit protein synthesis. Therefore, protein synthesis yield under feeding solution truly characterizes membrane-bound gene expression in microwells.

In this article, we used standard microfabrication techniques to make a novel microfluidic chip that hosts thousands of identical TXTL reactions sealed by a phospholipid membrane, offering larger and more homogeneous statistics than usual membrane-bound cell-free gene expression configurations, such as liposomes,<sup>3,7,8,10,11</sup> using a protocol that allows filling all the microwells with only a fraction of a microliter of reaction mix (Figure 5C). Cell-free gene expression in those microwells revealed a high protein synthesis yield of about 1.0 mg/mL, comparable to previously reported values in TXTL systems,<sup>3–5,22</sup> and far superior to that obtained in emulsions<sup>9,18,32</sup> or microwells sealed by a solid substrate<sup>13–18,27–29</sup> (Figure 5C). By combining these technical advantages, the present study finally reports the novel effect of the composition of the outer medium, not only on microreactors durability, but also on the efficiency of cell-free gene expression (Figure 5C). In addition, large statistics of gene expression yield shows non-Gaussian distribution that is also found in a clonal population of living cells.<sup>30</sup> Because the fluctuation of DNA copy number ( $\approx 2\%$ ) in our device is too low to explain such a distribution of protein synthesis yield, a long-tail distribution under feeding solution is an intrinsic aspect of complex reaction cascades.<sup>31,32</sup>

The membrane is a crucial component in the design of artificial cells. Given the importance of bilayer membranes in interfacial functionalization, this approach could be useful to

study membrane proteins expressed in TXTL such as  $\alpha$ -hemolysin,<sup>3,33</sup> Sec-translocon,<sup>34</sup> and cell division machineries.<sup>10,11,35</sup> In the future, a cell-free gene expression controlled by boundary geometry will also provide novel insight in the design principles of minimal cells in the form of bioreactors with functional membrane interface.

## MATERIALS AND METHODS

**Chemical Reagents.** The reaction mix contained 9  $\mu\text{L}$  of extracted medium (myTXTL, Arbor Bioscience), 3  $\mu\text{L}$  of  $P_{70a}$ -deGFP<sup>5</sup> plasmid DNA at 35 ng/ $\mu\text{L}$  (final concentration 3.5 nM), and 0.5  $\mu\text{L}$  of Rhodamine-BSA at 50 mg/mL (final concentration 30  $\mu\text{M}$ ), replaced with distilled water when no volume marker is used.

The oil phase consists of phospholipid (DOPE and DOPG, Avanti Polar Lipids) dissolved at 0.2 wt % each in light mineral oil and sonicated at 60  $^{\circ}\text{C}$  for 1 h. An 11  $\mu\text{L}$  sampling of DOPE-ATTO-594 (Funakoshi) at 0.53 mg/mL in an 8:2 mixture of chloroform/methanol was dried and supplemented with 300  $\mu\text{L}$  of oil phase to prepare the labeled oil phase with fluorescent DOPE at 0.5 mol %.

The feeding solution was made according to previous study.<sup>21</sup> Simplified buffer is an inert solution of ions typically present in biological media (potassium acetate at 100 mM), polyethylene glycol polymer (molecular weight  $\approx 20$  kDa, at 20 wt %, Alfa Aesar), and fatty acid (octadecanoic acid at 240  $\mu\text{mol/L}$ , NU Check Prep) dissolved in a pH 8.5 solution (Tris-HCl 6.6 mM).

If not specified otherwise, chemical compounds were purchased from Sigma-Aldrich.

**Microfluidic Chip.** Glass cover slides (Matsunami) were cleaned (1-day bath in a 10% Ace detergent solution followed by a 1-day bath of isopropyl alcohol, both purchased from Asone) and used as substrate for photoresist SU-8 3025 (Microchem) that was spin-coated to a 30  $\mu\text{m}$  thickness. The design—printed in a chromium mask (Mitani micronics)—was shone into the photoresist with a mask aligner by conventional photolithography techniques, then developed with an SU-8 developer (Microchem). The depth of the microwells was measured with a laser profiler (Keyence). To increase the wettability contrast between the inside and the outside of the microwell, CYTOP (AGC chemicals) was coated on the array of microwells with a spin-coater (3000 rpm for 30 s, then 1 h at 95 °C) to a thickness less than 1  $\mu\text{m}$ .

The PDMS cover was made with conventional soft lithography techniques. The master was made of a 50  $\mu\text{m}$ -thick pattern of SU-8 3025 spin-coated on a silicon wafer (Matsuzaki). A 9:1 mixture of PDMS polymer and curing agent (Sylgard 184, Dow Corning) was cast on the master, and left to cure at 70 °C for 1 h. After trimming the PDMS cap, holes were punched at the inlet and outlets with a 1 mm hole puncher.

The microfluidic chip was assembled with plasma-activated bonding of the PDMS cover onto a glass slide with CYTOP-coated SU8 microwells. The naked glass surface was exposed 10 s to a corona discharge (SHINKO Denso). The hydrophobicity of the CYTOP coating declines with plasma activation and was thus protected. The PDMS cap was activated in a plasma cleaner (Harrick, PDC-32G) at high intensity for 30 s. Alignment was performed under a binocular loupe (NIKON). Bonding was completed after 1 h at 95 °C.

Bulk experiments were conducted between a glass cover slide and a glass coverslip separated by a 30  $\mu\text{m}$  double sided adhesive tape spacer (KGC Chemical).

**Optical Microscopy and Image Analysis.** Cell-free TXTL reactions were observed with an inverted fluorescent microscope (Olympus IX73) at 20 $\times$  magnification. Time-lapsed images were recorded every 5 min for 24 h with a cMOS camera (Andor Neo5.5). An LED light source (XLED1, Lumendynamics) provided fluorescent excitation. Green laser light (Cobolt, 532 nm, 50 mW) was used for FRAP analysis. Quantitative image analysis was done using custom MATLAB scripts.

**Filling Protocol.** Ten microliters of reaction mix was injected with a micropipette in the chamber and kept at 350 mbar with a pressure controller (Fluigent) until no air remained. This step takes up to 30 min. After the air was removed from the chamber, the oil phase was injected at 200 mbar until all the microwells filled with reaction mix were covered with oil. Finally, the external buffer was injected at 200 mbar. Altogether, these two last steps take around a minute.

## ■ ASSOCIATED CONTENT

### 📄 Supporting Information

The Supporting Information is available free of charge on the ACS Publications website at DOI: 10.1021/acssynbio.9b00247.

Figures describing microreactors under simplified buffer, correlation between yield and reaction time of protein synthesis, distributions of membrane thickness, detail of

the model of gene expression in cell-free extract with leaky membrane, and reaction mix calibration (PDF)

## ■ AUTHOR INFORMATION

### Corresponding Author

\*E-mail: ziane.izri@phys.kyushu-u.ac.jp.

### ORCID

Ziane Izri: 0000-0003-4074-1535

Vincent Noireaux: 0000-0002-5213-273X

### Notes

The authors declare no competing financial interest.

## ■ ACKNOWLEDGMENTS

We thank A. Libchaber and R. Sakamoto for discussion, and K. Tabata and H. Noji for microfabrication at the early stage of this study. This work was supported by Human Frontier Science Program Research Grant (RGP0037/2015), Grant-in-Aid for Scientific Research on Innovative Areas (JP16H00805 Synergy of Structure and Fluctuation, JP17H05234 Hadean Bioscience, and JP18H05427 Molecular Engines), and Grant-in-Aid for Scientific Research (B) JP17KT0025 from MEXT.

## ■ REFERENCES

- (1) Noireaux, V., Maeda, Y. T., and Libchaber, A. (2011) Development of an artificial cell, from self-organization to computation and self-reproduction. *Proc. Natl. Acad. Sci. U. S. A.* 108, 3473–3480.
- (2) Shimizu, Y., Inoue, A., Tomari, Y., Suzuki, T., Yokogawa, T., Nishikawa, K., and Ueda, T. (2001) Cell-free translation reconstituted with purified components. *Nat. Biotechnol.* 19, 751–755.
- (3) Noireaux, V., and Libchaber, A. (2004) A vesicle bioreactor as a step toward an artificial cell assembly. *Proc. Natl. Acad. Sci. U. S. A.* 101, 17669–17674.
- (4) Shin, J., and Noireaux, V. (2012) An *E. coli* cell-free expression toolbox: application to synthetic gene circuits and artificial cells. *ACS Synth. Biol.* 1, 29–41.
- (5) Garamella, J., Marshall, R., Rustad, M., and Noireaux, V. (2016) The All *E. coli* TX-TL toolbox 2.0: a platform for cell-free synthetic biology. *ACS Synth. Biol.* 5, 344–355.
- (6) Karzbrun, E., Shin, J., Bar-Ziv, R. H., and Noireaux, V. (2011) Coarse-grained dynamics of protein synthesis in a cell-free system. *Phys. Rev. Lett.* 106, 048104.
- (7) Nourian, Z., Roelofsen, W., and Danelon, C. (2012) Triggered gene expression in fed-vesicle micro-reactors with a multifunctional membrane. *Angew. Chem., Int. Ed.* 51, 3114–3118.
- (8) Deng, N.-N., Vibhute, M. A., Zheng, L., Zhao, H., Yelleswarapu, M., and Huck, W. T. S. (2018) Macromolecularly crowded protocells from reversibly shrinking monodisperse liposomes. *J. Am. Chem. Soc.* 140, 7399–7402.
- (9) Sakamoto, R., Noireaux, V., and Maeda, Y. T. (2018) Anomalous scaling of gene expression in confined cell-free reactions. *Sci. Rep.* 8, 7364.
- (10) Maeda, Y. T., Nakadai, T., Shin, J., Uryu, K., Noireaux, V., and Libchaber, A. (2012) Assembly of MreB filaments on liposome membranes: a synthetic biology approach. *ACS Synth. Biol.* 1, 52–59.
- (11) Furusato, T., Horie, F., Matsubayashi, H. T., Amikura, K., Kuruma, Y., and Ueda, T. (2018) De novo synthesis of basal bacterial cell division proteins FtsZ, FtsA, and ZipA inside giant vesicles. *ACS Synth. Biol.* 7, 953–961.
- (12) Borkowski, O., Bricio, C., Murgiano, M., Rothschild-Mancinelli, B., Stan, G.-B., and Ellis, E. (2018) Cell-free prediction of protein expression costs for growing cells. *Nat. Commun.* 9, 1457.
- (13) Karig, D. K., Jung, S.-Y., Srijanto, B., Collier, C. P., and Simpson, M. L. (2013) Probing cell-free gene expression noise in femtoliter volumes. *ACS Synth. Biol.* 2, 497–505.

- (14) Caveney, P. M., Norred, S. E., Chin, C. W., Boreyko, J. B., Razoooky, B. S., Retterer, S. T., Collier, C. P., and Simpson, M. L. (2017) Resource sharing controls gene expression bursting. *ACS Synth. Biol.* 6, 334–343.
- (15) Pardatscher, G., Schwarz-Schilling, M., Daube, S. S., Bar-Ziv, R. H., and Simmel, F. C. (2018) Gene expression on DNA biochips patterned with strand-displacement lithography. *Angew. Chem., Int. Ed.* 57, 4783–4786.
- (16) Karzbrun, E., Tayar, A. M., Noireaux, V., and Bar-Ziv, R. H. (2014) Programmable on-chip DNA compartments as artificial cells. *Science* 345, 829–832.
- (17) Tayar, A. M., Karzbrun, E., Noireaux, V., and Bar-Ziv, R. H. (2015) Propagating gene expression fronts in a one-dimensional coupled system of artificial cells. *Nat. Phys.* 11, 1037–1041.
- (18) Dittrich, P. S., Jahnz, M., and Schwille, P. (2005) A new embedded process for compartmentalized cell-free protein expression and on-line detection in microfluidic devices. *ChemBioChem* 6, 811–814.
- (19) Vaish, A., Guo, S., Murray, R. M., Grandsard, P. J., and Chen, Q. (2018) On-chip membrane protein cell-free expression enables development of a direct binding assay: A curious case of potassium channel KcsA-Kv1.3. *Anal. Biochem.* 556, 70–77.
- (20) Watanabe, R., Soga, N., Fujita, D., Tabata, K. V., Yamauchi, L., Kim, S. H., Asanuma, D., Kamiya, M., Urano, Y., Suga, H., and Noji, H. (2014) Arrayed lipid bilayer chambers allow single-molecule analysis of membrane transporter activity. *Nat. Commun.* 5, 4519.
- (21) Watanabe, R., Soga, N., Yamanaka, T., and Noji, H. (2015) High-throughput formation of lipid bilayer membrane arrays with an asymmetric lipid composition. *Sci. Rep.* 4, 7076.
- (22) Caschera, F., and Noireaux, V. (2014) Synthesis of 2.3 mg/mL of protein with an all *Escherichia coli* cell-free transcription-translation system. *Biochimie* 99, 162–168.
- (23) Nagle, J. F., Mathai, J. C., Zeidel, M. L., and Tristram-Nagle, S. (2008) Theory of passive permeability through lipid bilayers. *J. Gen. Physiol.* 131, 77–85.
- (24) Williams, J., and Shaykewich, C. F. (1969) An evaluation of Polyethylene glycol (P.E.G.) 6000 and P.E.G. 20,000 in the osmotic control of soil water matric potential. *Can. J. Soil Sci.* 49, 397–401.
- (25) Budin, I., and Szostak, J. W. (2011) Physical effects underlying the transition from primitive to modern cell membranes. *Proc. Natl. Acad. Sci. U. S. A.* 108, 5249–5254.
- (26) Dervaux, J., Noireaux, V., and Libchaber, A. J. (2017) Growth and instability of a phospholipid vesicle in a bath of fatty acids. *Eur. Phys. J. Plus* 132, 284.
- (27) Okano, T., Matsuura, M., Kazuta, Y., Suzuki, H., and Yomo, T. (2012) Cell-free protein synthesis from a single copy of DNA in a glass microchamber. *Lab Chip* 12, 2704–2711.
- (28) Okano, T., Matsuura, M., Suzuki, H., and Yomo, T. (2014) Cell-free protein synthesis in a microchamber revealed the presence of an optimum compartment volume for high-order reactions. *ACS Synth. Biol.* 3, 347–352.
- (29) Kim, S. H., Yoshizawa, S., Takeuchi, T., Fujii, T., and Fourmy, D. (2013) Ultra-high density protein spots achieved by on chip digitalized protein synthesis. *Analyst* 138, 4663.
- (30) Salman, H., Brenner, N., Tung, C., Elyahu, N., Stolovicki, E., Moore, L., Libchaber, A., and Braun, E. (2012) Universal protein fluctuations in populations of microorganisms. *Phys. Rev. Lett.* 108, 238105.
- (31) Smits, W. K., Kuipers, O. P., and Veening, J.-W. (2006) Phenotypic variation in bacteria: the role of feedback regulation. *Nat. Rev. Microbiol.* 4, 259–271.
- (32) Sunami, T., Hosoda, K., Suzuki, H., Matsuura, T., and Yomo, T. (2010) Cellular compartment model for exploring the effect of the lipidic membrane on the kinetics of encapsulated biochemical reactions. *Langmuir* 26, 8544–8551.
- (33) Fujii, S., Matsuura, T., Sunami, T., Kazuta, Y., and Yomo, T. (2013) In vitro evolution of  $\alpha$ -hemolysin using a liposome display. *Proc. Natl. Acad. Sci. U. S. A.* 110, 16796–17801.
- (34) Matsubayashi, H., Kuruma, Y., and Ueda, T. (2014) *In vitro* synthesis of the *E. coli* Sec translocon from DNA. *Angew. Chem., Int. Ed.* 53, 7535–7538.
- (35) Loose, M., Fischer-Friedrich, E., Ries, J., Kruse, K., and Schwille, P. (2008) Spatial regulators for bacterial cell division self-organize into surface waves *in vitro*. *Science* 320, 789–792.

## Supplemental information for

### Gene expression in *on-chip* membrane-bound artificial cells

Ziane Izri<sup>1,\*</sup>, David Garenne<sup>2</sup>, Vincent Noireaux<sup>2</sup>, and Yusuke T. Maeda<sup>1</sup>

<sup>1</sup>Department of Physics, Kyushu University, Fukuoka 819-0395, Japan

<sup>2</sup>Department of Physics and Astronomy, Minnesota University, Minneapolis, MN 55455 USA

\*corresponding address: [ziane.izri@phys.kyushu-u.ac.jp](mailto:ziane.izri@phys.kyushu-u.ac.jp)

### Supplementary figures

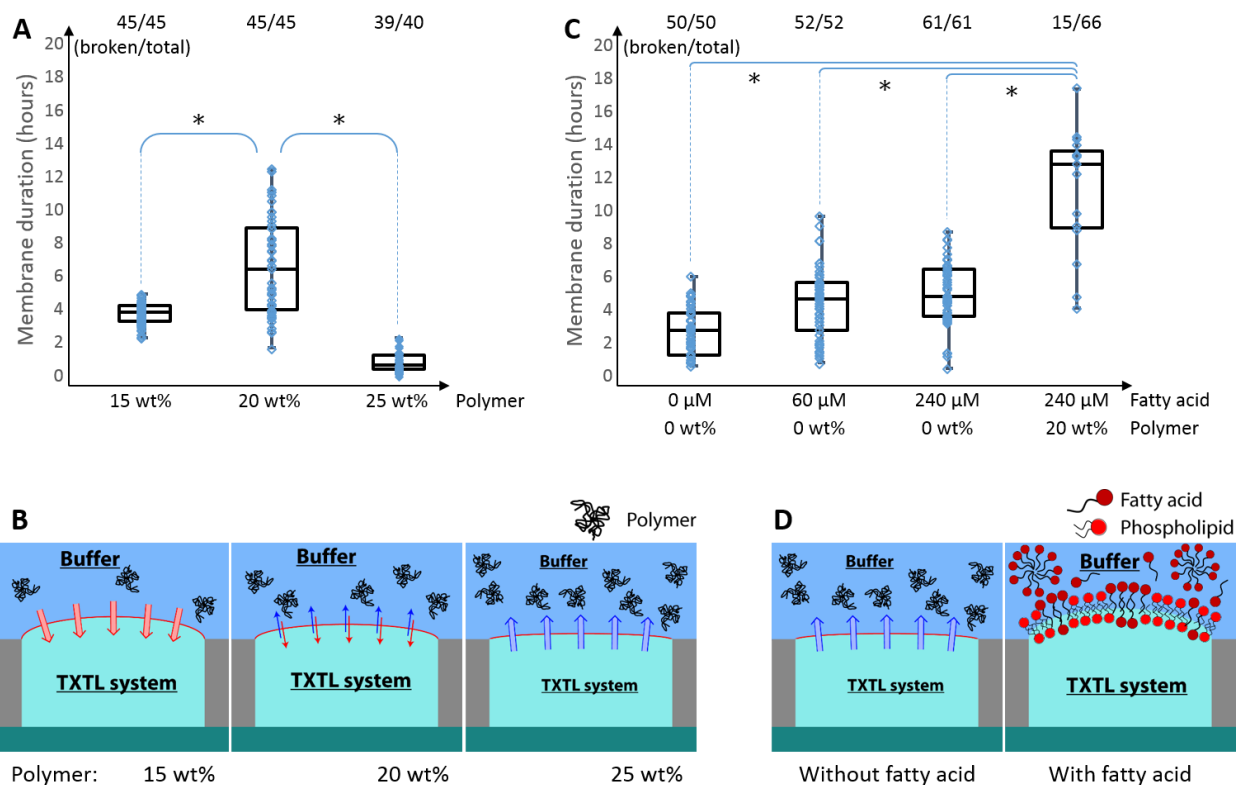


**Figure S1:** Polymer and fatty acid micelles in the external buffer stabilize membrane. (A) Membrane duration affected by osmotic stress from various concentrations of inert polymer in external buffer. While it is inexistent at 20wt%, the osmotic flow reduces the lifetime of the membrane. (B) Enhancement of membrane duration in the presence of polymer. At 15wt% (left), the outer medium is hypotonic, isotonic at 20wt% (middle) and hypertonic at 25wt% (right). (C)

Membrane duration at various concentrations of fatty acid and polymer in external buffer. To further increase the stability of the membrane, fatty acid is added in the simplified buffer at a concentration that allows a stable growth of the membrane in case of slightly non-isotonic conditions. The addition of fatty acid alone moderately increases the lifetime of the membrane as it helps generate extra membrane surface under osmotic stress. Together with the presence of polymer at isotonic concentration, it significantly increases the lifetime of the membrane. (C far right). (D) The integration of fatty acid at the membrane interface at moderate concentration allows the stable growth of the phospholipid membrane. By the end of the continuous observation, all the membranes broke, except for simplified buffer containing both polymer and fatty acid (ratios at top of A and C).

The *U-test* for all the pairs of samples enclosed under horizontal brackets gives a *p-value*  $< 10^{-5}$ , showing a strict increase in life expectancies among the pairs considered.

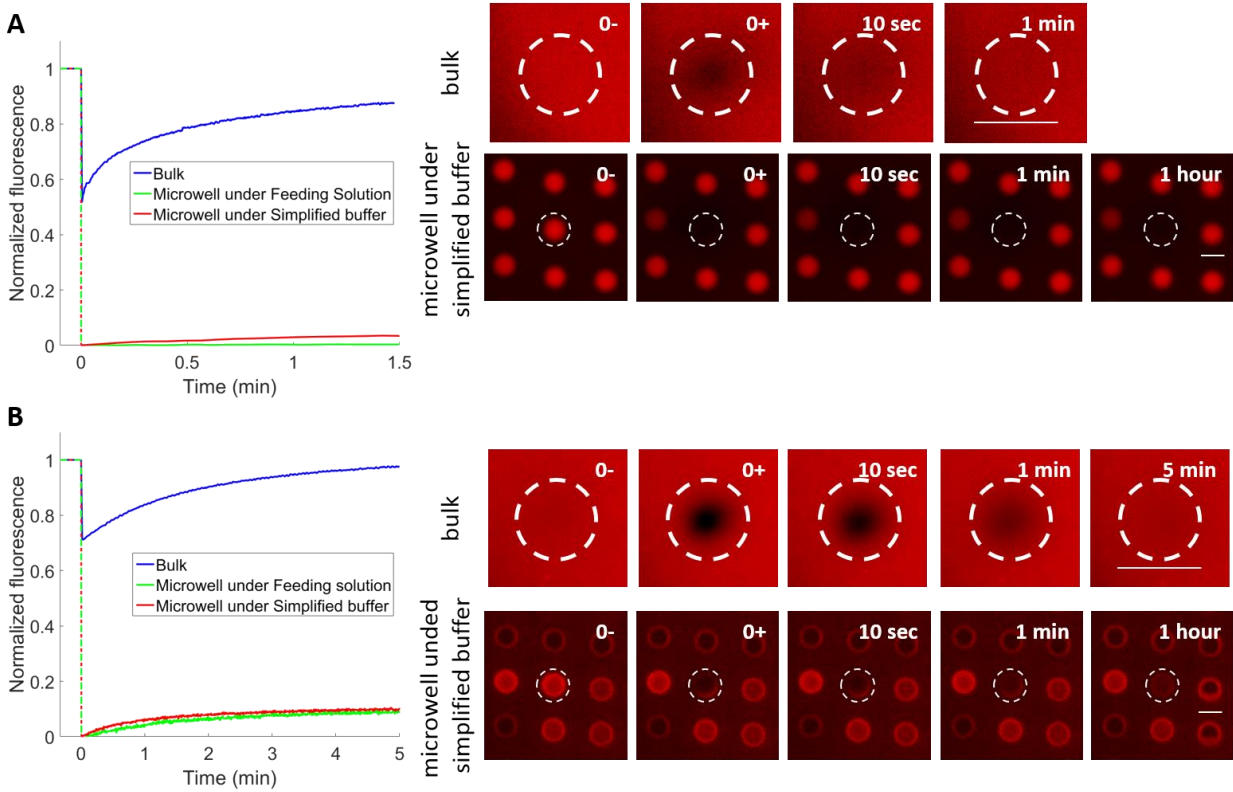


**Figure S2:** FRAP analysis to visualize insulation of microwells under simplified buffer. (A) The leakage of TXTL system from inside microwells was tested with the FRAP analysis of the volume marker in microwells. In microwells (red solid line) it is less than a few percent within 1.5 minute, similarly to micro-reactors under feeding solution (green solid line). Snapshots of FRAP (right). In the top snapshot panel, the white dashed line encloses the photo-bleached area in a bulk experiment, while in the bottom snapshot panel, the white dashed circle encloses the only photo-bleached microwell in the array. (B) The insulation of microwell membrane under simplified buffer was tested with the FRAP analysis of membrane marker. In microwells (red solid line) it is less than a few percent within 5 minutes, similarly to micro-reactors under feeding solution (green solid line). Snapshots of FRAP (right). In the top snapshot panel, the white dashed line encloses the photo-bleached area in a bulk experiment. While in the bottom snapshot panel, the white dashed circle encloses the only photo-bleached micro-reactor in the array. Scale bars are 25  $\mu\text{m}$ .

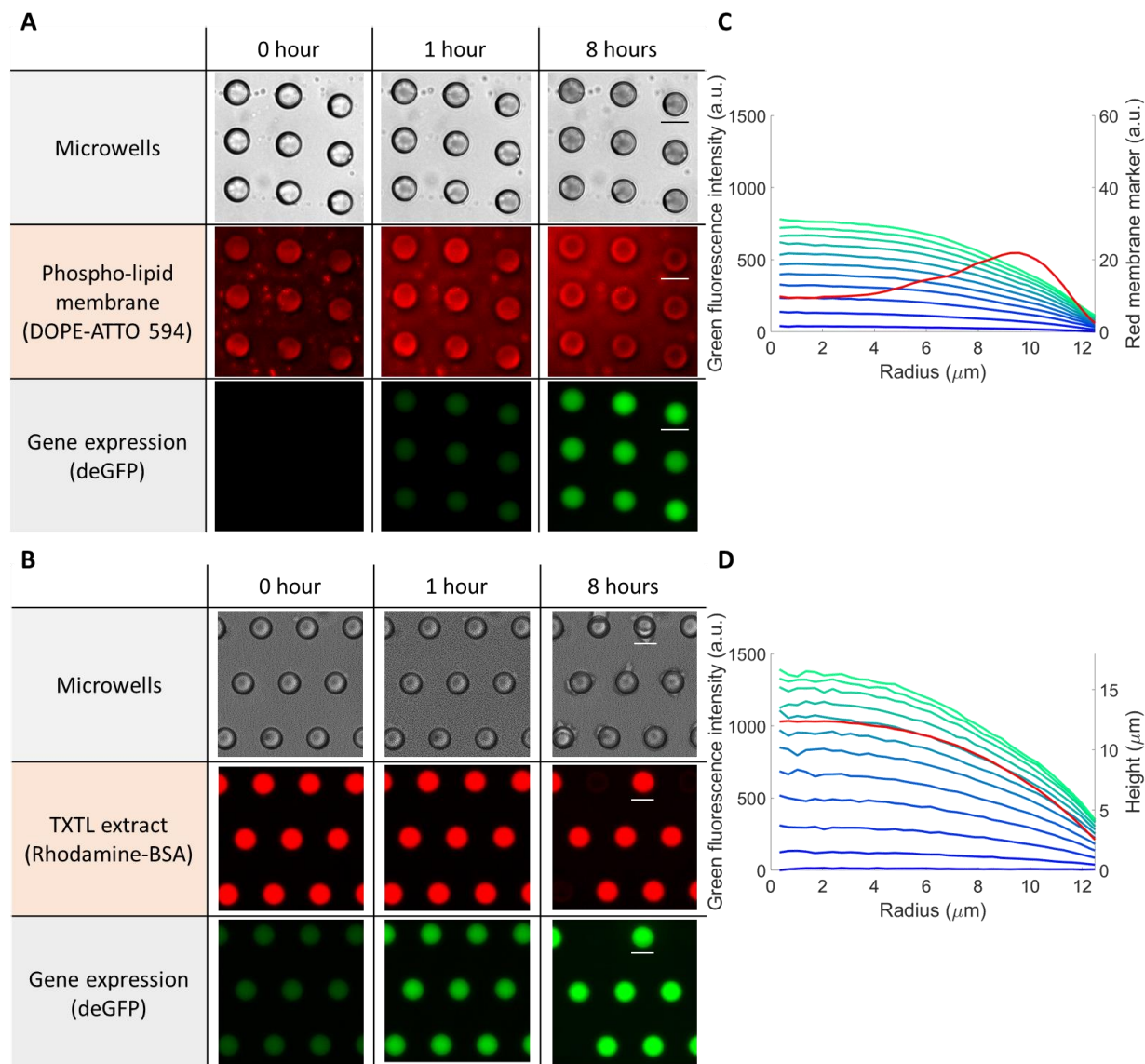


**Figure S3:** Typical observations of micro-reactors. (A and B) Snapshots over 8 hours of TXTL reactions of deGFP synthesis under simplified buffer. Phospholipid membrane is visible in bright field (A and B, top). As membranes break, the oil trapped at the membrane interface is released and spreads over the CYTOP-coated surface surrounding the microwell (B top right). The red fluorescence of microwells remains constant until the membrane breaks (A and B, middle). deGFP is synthesised and the green fluorescence intensities of the micro-reactors increases (A and B, bottom). (C and D) Radial distributions of green fluorescence intensity over 8 hours of gene expression (from blue to green) as well as red fluorescence intensity (red), for membrane marker (C) and volume marker (D). Scale bars are 25  $\mu\text{m}$ .

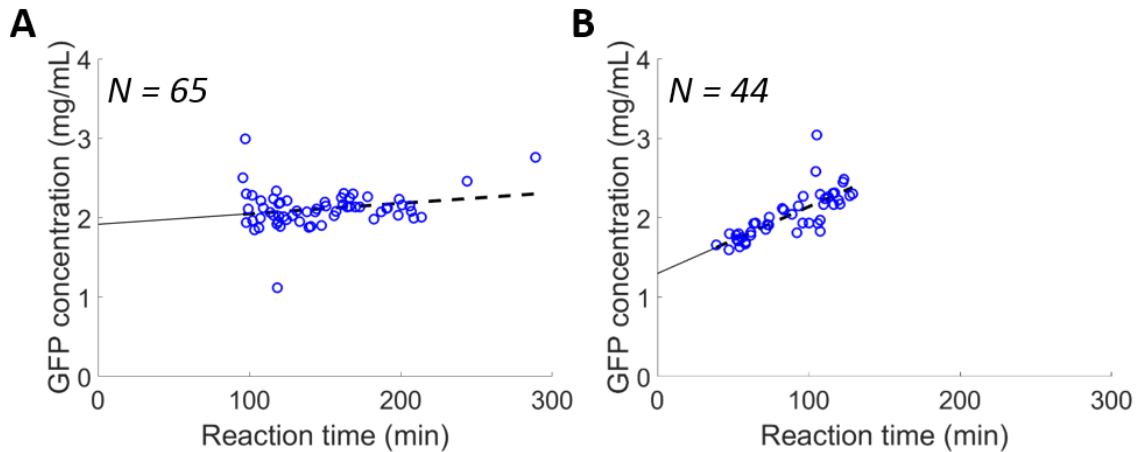


**Figure S4:** Relation between the reaction time and the yield of protein synthesis (extracted from fitting parameters) under (A) feeding solution and (B) simplified buffer, over the respective samples kept under continuous observation. From model of gene expression in cell-free extract with leaky membrane, reaction time for gene expression unaffected by leak should be longer than under the effect of a leak of nutrients. Gene expression is twice longer under feeding solution than under simplified buffer. In addition, final GFP concentration is expected to increase with reaction time under the effect of a leak. The yield of protein synthesis is independent from reaction time under feeding solution, but increases with reaction time under simplified buffer. These two observations show that gene expression under simplified buffer is affected by a leak of nutrients, whereas under feeding solution, no leak affects gene expression. N counts the number of micro-reactors observed in each case.

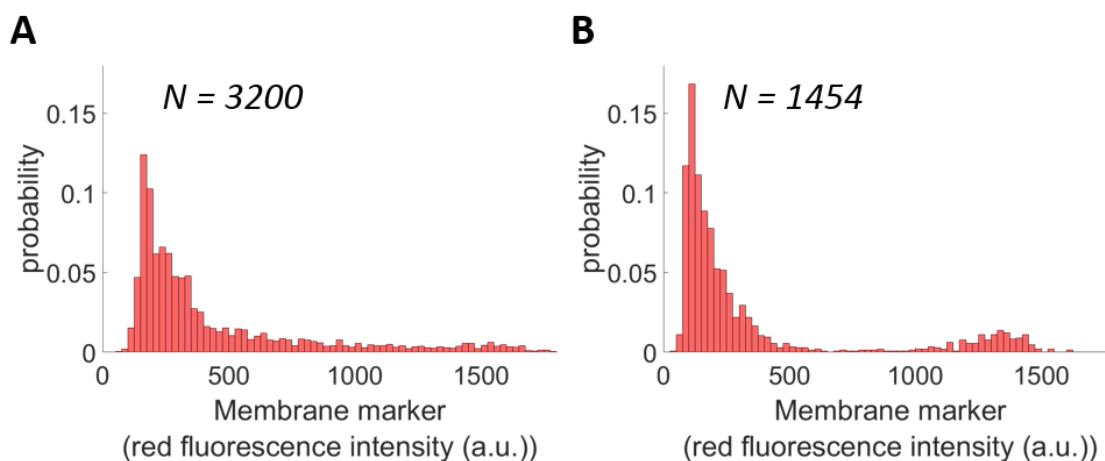


**Figure S5:** Distribution of membrane marker fluorescence intensities under (A) feeding solution and (B) simplified buffer, collected from intact micro-reactors after 24 hours of gene expression. Although both distributions show a sharp peak at low values intensities, representing individual membranes, these maxima are met at a larger value under feeding solution (~150 a.u.) than under simplified buffer (~100 a.u.). This difference in typical fluorescence intensity indicates that membranes are thicker under feeding solution than under simplified buffer. In addition, thickness distribution is broader under feeding solution (standard deviation ~ 200 a.u.) than under simplified buffer (standard deviation ~ 100 a.u.). As simplified buffer is more viscous than feeding solution, less oil is trapped at the interface with simplified buffer. N counts the number of micro-reactors observed in each case.

## Supplementary text

### Model of gene expression in cell free extract with leaky membrane

Assuming that the rate of production of deGFP (concentration  $c(t)$ ) is proportional to the amount of substrate  $S(t)$ , with a characteristic time  $\tau$  and a stoichiometry coefficient  $n$  we have:

$$\frac{dc}{dt} = \frac{1}{n} \frac{S}{\tau} \cdot \cdot \cdot (2)$$

As a result of protein synthesis, the substrate is consumed with the same time constant  $\tau$ . In addition, it is also depleted at a time scale  $\tau'$  under the action of the leak to the external buffer, assumed empty of substrate at all times, which gives :

$$\frac{dS}{dt} = -\frac{S}{\tau} - \frac{S}{\tau'} \cdot \cdot \cdot (3)$$

We then easily find the exponential decay of the amount of available substrate with a characteristic time  $T$ :

$$S(t) = S_0 \exp(-t/T) \cdot \cdot \cdot (4)$$

with

$$1/T = 1/\tau + 1/\tau' \cdot \cdot \cdot (5)$$

and  $S_0$  the initial amount of the substrate. The exponential increase of the amount of deGFP synthesized in the micro-reactor is then:

$$c(t) = c_\infty [1 - \exp(-t/T)] \cdot \cdot \cdot (6)$$

with

$$c_\infty = \frac{S_0 T}{n \tau} \cdot \cdot \cdot (7)$$

The concentration of protein in micro-reactors follows a kinetics driven by the rate of depletion of substrate, with a characteristic time constant  $T = \frac{\tau\tau'}{\tau + \tau'}$ , and a final concentration  $c_\infty = \frac{S_0}{n} \frac{\tau'}{\tau + \tau'}$ . When leak is negligible ( $\tau' \gg \tau$ ), the time scale of the protein synthesis equals that of substrate consumption  $\tau$ , and the yield of protein synthesis reaches  $\frac{S_0}{n}$ , independent from the time scale of the protein synthesis. However, as substrate leak increases,  $\tau'$  decreases, and both the yield  $c_\infty$  and the reaction time  $T$  of the protein synthesis decrease. Conversely, an increase in the reaction time goes with an increase of the yield.

### **Measurement of height profile in micro-reactors**

Average height of micro-reactors was obtained from average volume marker fluorescence intensity over the surface of each micro-reactor, after calibrating it with several known heights and subtracting background intensity. Same calibration was performed with purified GFP at 0.7 mg/mL. Then, protein concentration was obtained from the ratio of the average green fluorescence over the average of red fluorescence over the surface of each micro-reactor, after subtracting background intensity and using both previous calibrations.